Title
Imaging of Biomolecules with Scanning Tunneling Microscope: Problems and Prospects

Journal
Journal of vacuum science and technology A, 8(1)

Authors
Salmeron, E.M.
Beebe, T.
Odriozola, J.
et al.

Publication Date
1989-07-01

LBL-27566
Preprint

Center for Advanced Materials

CAM

Submitted to Journal of Vacuum Science
and Technology A

Imaging of Biomolecules with the Scanning Tunneling Microscope: Problems and Prospects

M. Salmeron, T. Beebe, J. Odriozola, T. Wilson,
D.F. Ogletree, and W. Siekhaus

July 1989

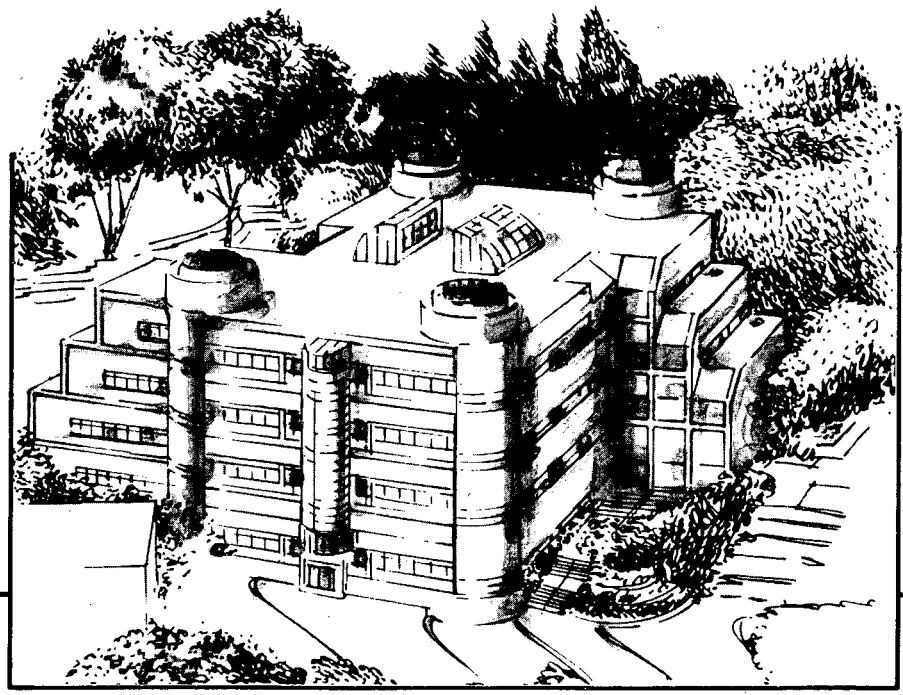

Materials and Chemical Sciences Division

Lawrence Berkeley Laboratory • University of California

ONE CYCLOTRON ROAD, BERKELEY, CA 94720 • (415) 486-4755

Prepared for the U.S. Department of Energy under Contract DE-AC03-76SF00098

DISCLAIMER

LBL-27566

Imaging of Biomolecules with the Scanning Tunneling Microscope: Problems and Prospects

M. Salmeron*, T. Beebe#a, J. Odriozola*b,
T. Wilson#, D.F. Ogletree*, and W. Siekhaus#

* Center for Advanced Materials
Materials and Chemical Sciences Division
Lawrence Berkeley Laboratory
1 Cyclotron Road
Berkeley, CA 94720

and

Lawrence Livermore National Laboratory
700 East Avenue
Livermore, CA 94550

July 1989

Permanent Address:

a Dept. of Chemistry; University of Utah; 1400 E 2nd South Street Salt Lake City, UT 84112

b Dept. de Quimica Inorganica; Instituto de Ciencia de Materiales; Universidad de Sevilla; 41012-Sevilla; Spain

IMAGING OF BIOMOLECULES WITH THE SCANNING TUNNELING MICROSCOPE: PROBLEMS AND PROSPECTS.

by

M. Salmeron (*), T. Beebe[a] (#), J. Odriozola[b] (*),
T. Wilson (#), D.F. Ogletree (*) and W. Siekhaus (#).

Lawrence Berkeley Laboratory (*)

and

Lawrence Livermore National Laboratory (#).

ABSTRACT

The capabilities of the Scanning Tunneling Microscope as a tool to study the morphology and structure of adsorbed biomolecules are reviewed in view of recent experimental results. Problems such as electrical conductivity of the biomolecules, fixation to the substrate and identification are analyzed in detail. In particular the role of tip-surface interaction giving rise to repulsive forces is illustrated. It is concluded that fixation rather than conductivity is the major obstacle to the use of the STM for biological imaging.

Key words: DNA, deoxyribonucleic acid, STM, scanning tunneling microscope

1. INTRODUCTION

The exploration of the capabilities of the Scanning Tunneling Microscope (STM) to image biological material started soon after the invention of the instrument. From the first results by Baro et al. in 1985 [1], till the recent reports by Arscott et al. [15] in June 1989, more than 20 papers have been devoted to this effort. In spite of the promise of high resolution and simplicity of operation, researches are still exploring the conditions in which STM can be applied to biology. This is because the interaction of the instrument and the biological material is not yet fully understood and consequently, techniques for adequate sample preparation are still being developed. In the field of Transmission Electron Microscopy (TEM), many years were necessary to develop effective preparation techniques. These include preparation of thin transparent carbon substrates, metal shadowing procedures to enhance contrast etc.

It is the purpose of this paper to identify and discuss some of the problems that are specific to STM and to illustrate these with results obtained while imaging DNA deposited on graphite in the author's laboratory. We have grouped these problems into three categories. The first and most widely mentioned is that of electrical conductivity. It has been argued repeatedly that most biological material is electrically insulating in the bulk and that this will prevent the use of techniques that require the passage of current like

the STM. To circumvent this problem many researches have borrowed traditional methods used in TEM consisting of metal shadowing the specimens [2,4,7,8,13,19]. The second one is the problem of fixation of the biomaterial to the substrate. More specifically, due to strong tip-molecule interactions, the question is can displacement and perhaps modification of the weakly bound adsorbates be prevented?. Another category of problems include the identification of the imaged structures. Ideally, some type of spectroscopy, like detection of electronic states or vibrational modes should allow unambiguous analysis. Since this possibility has not yet been demonstrated, most researches resort to geometrical identification by shape and size of the observed objects. This is a less perfect method and care must be taken to sort out a variety of possible artifacts.

We will illustrate many of these problems by presenting an extended account of our work on DNA deposited on graphite. We will then discuss in detail the various problems mentioned.

2. EXPERIMENTAL

2.1 Preparation of DNA samples

Several DNA preparations were used in this work. High molecular weight calf thymus DNA (Worthington Biochemical Corporation) was dissolved in aqueous 10 mM KCl solution. Aliquots of this solution were diluted with 10 mM KCl to working concentrations of 1 mg/ml and sometimes 0.05 mg/ml. DNA from bacteriophage T4 was also used. It was maintained in 5 mM Tris-HCl (pH = 7.1), 1 mM $MgSO_4$, and 0.5 M NaCl, at a concentration of 0.23 mg/ml. In some cases a dilute droplet of the detergent Sodium Dodecyl Sulfate (SDS), was added to promote uniform spreading of the DNA on the highly oriented pirolytic graphite (HOPG) substrate.

The HOPG sample was cleaved in air prior to all depositions. A droplet of the solution containing DNA was transferred by micropipet onto the HOPG surface. Using gentle warming in some cases, and simple room temperature drying in others, the water was allowed to evaporate as checked by visual inspection. This process left behind a series of concentric rings, increasing in concentration to a thick crusty deposit in the center. Blank droplets containing no DNA, but the same salt concentration left only a barely visible speck of KCl in the center. We observed that a stable tunnel junction could not be established in

regions where the deposit was visibly thick, and intentionally avoided these regions when positioning the tip within tunneling range on the sample. The outer edges where imaging was done appeared smooth, but somewhat dull in luster. In some cases, the excess solution on the surface was removed by capillary absorption using filter paper.

2.2. Microscope design and data acquisition.

Two different STM heads were used in this study that yielded similar results. The first consists of a single tubular piezo with micrometer driven differential deflection bars for coarse approach. It is similar to a previously described tripod design [20]. In the second microscope, two coaxial piezo tubes are employed, and coarse sample motion is accomplished by inertial translation of the sample using the outer tube [21,27]. STM control electronics and image acquisition and processing software of our own design were employed [22]. All the images presented here are constant current topographic images and only raw unprocessed data are used unless specifically noted, in which case a simple 3x3 point weighted smoothing was applied. Heights are represented in false color according to the gray scale shown in the figures. The images consist of 256x256 data points obtained with tip velocities between 1000 and 4000 A/s. Bias voltages below 0.3 V were used in both polarities with no observable differences except where indicated. Gap resistances varied between 1 and 100 Mohm.

Our tips were made by simply mechanically cutting a Pt-Rh alloy wire of 1 mm diameter.

3. RESULTS

3.1 Morphology of the graphite surface.

We have collected a large number of STM images of both DNA deposited onto graphite and graphite without any molecules being intentionally deposited. The latter "blank" experiments can be divided into two groups: surfaces which have been cleaved with nothing subsequently deposited, and surfaces which have been cleaved followed by deposition of a droplet containing the salt solution but not containing DNA. The images produced from both of these types of blank experiments were similar. In most of the surfaces produced by cleavage, there is no structure seen over square areas of several thousand Angstroms side. However, in some cases the surface exhibits varying degrees of disruption. An example of such an image is figure 1a which shows a large area of a HOPG surface with a step of two atoms height along with a "kink" area where the material from the terrace has been folded back on top of itself. Another disrupted area is shown in figure 1b, where detached flakes are observed of several hundred Angstroms width and only a few atomic layers height. There are plenty of examples of these types of structures for surfaces which have had nothing deposited, surfaces which have had only salt solution deposited, and surfaces which have had salt solution plus DNA deposited.

An example of potentially misleading structures arising from HOPG is given in figure 2a. Although nothing was deposited on the surface, considerable fine structure is observed on the step edges running diagonally across the image. Similar types of structure are occasionally observed also when DNA was deposited. This is shown in the example of figure 2b corresponding to a sample with bacteriophage T4 DNA deposited. The edges of triangular flakes can be seen that display again remarkable periodicity. The periodicity of these edge structures ranges from 20 to 80 A. Often they display angular bends of 60 or 120 degrees within the field of the image, reflecting the graphite symmetry. In our work with DNA we have avoided making interpretations about these kind of very linear geometric structures.

3.2 Tip-surface interaction.

When imaging chemically inert surfaces in air, considerable repulsive forces can be exerted between the tip and the surface for typical tunneling conditions (less than several hundred megohms gap resistance). This is particularly evident in the case of graphite where these forces can displace entire flakes during scanning. The example of figure 3a and b illustrate this effect very clearly. The 1000x1000 A images show a large terrace on the left side and a small flake of 150x250 A size that is moved from the right to the left of the image in the course of the scan. Smaller displacements take also place during scanning as shown by the discontinuities in the vertical direction (scan is horizontal). Part c of the figure shows another manifestation

of the tip-surface interaction. The tip was positioned of top of a small flake, roughly 200 A wide. Then a small area of 18x19 A was imaged. A dramatic elongation of the graphite unit cell is observed that we believe is due to the tip dragging the flake back and forth as it scans. These type of displacements were observed both with and without DNA deposited on the surface.

3.3 Observation of DNA in aggregates and defects.

After the results of the previous section it is not surprising that only large bundles of DNA forming crystals or amorphous structures, as well as DNA that is more strongly bound at defects such as step edges can be imaged with the STM.

We have obtained several images of large structures on surfaces onto which DNA was deposited, which are quite distinct from any of the geometric structures described above. These include bundles of high molecular weight DNA, twisted into fairly stable rafts. In another example crystalline structures with a cubic-like symmetry were obtained after depositing calf thymus DNA with a droplet of dilute SDS to enhance spreading on the HOPG. Finally stable clusters made of graphite flakes with decorated edges were also obtained after deposition of bacteriophage T4 DNA. Although large aggregates were found consistently on surfaces with deposited DNA, their interpretation is difficult at the present time.

Figure 4a-f shows the evolution of a few isolated DNA strands obtained by deposition of calf thymus DNA that appear to be anchored at the edges of graphite flakes. Horizontal displacements are observed in the oval-shaped flake in a), along with small modifications of the edge-bound DNA fragment (b and c). Other fragments that do not appear to be bound to edges of graphite are easily moved as shown on the lower left of 4a, bottom of 4b and left of the oval structure in 4c. Parts d) to f) were taken in the region immediately below (portions of the oval-shaped structure are still visible in the upper right corner of d) and e). The fragment at the bottom of d), e) and f) shows clearly the spiral helix pitch distances, and after turning over itself on the right hand side returns back to the left in a structure suggestive of supercoiling. A detailed account of this image has already been published [16]. Notice the small but noticeable modifications that take place in the successive images d) to f), where material sitting on top of the DNA strand in d) and e) has been displaced by the tip in f).

3.4 Electronic effects.

We attempted to investigate also how the images were affected by the bias voltage at which they were acquired. A series of images is shown in figure 5 a) to c), in which a circular structure formed after depositing calf thymus DNA was imaged at several different bias voltages and current setpoints, for electrons flowing from the sample to the tip. The contrast almost completely disappears when the bias voltage decreases from 100 to 10 mV. By returning the bias to the

original 100 mV, the level of contrast was only partially restored. Notice also the z-scale that changed from 62 to 13 A indicating permanent modification of the structure.

4. DISCUSSION

4.1 The problem of electrical conductivity.

From the results presented here and from the observations of other authors [1,3-6,8,9,14-18], it appears that in spite of the insulating character of bulk solid DNA, imaging by the STM of this and other biomolecules of similar non-conductive character is not a major problem, at least for deposits a few hundred Angstroms thick. This result can be explained by careful consideration of the transport process of the tunneling electrons from the tip, through the adsorbed molecule and to the substrate (or vice versa, for negative sample bias). The insulating character of bulk DNA and other organic molecules, is a result of the negligible overlap of electronic orbitals between neighboring molecules in the corresponding crystal. Electrons can only "hop" from molecule to molecule and this requires high activation energies. Electrons can also tunnel from molecule to molecule. The probability for many of these processes to occur sequentially in order to transport over large distances will thus decay very rapidly. Therefore the problem we want to analyze is that of an electron tunneling from the tip to a weakly adsorbed molecule, its propagation through the molecular potential well and its further tunneling to the substrate.

While a complete three dimensional calculation of the process is

not a trivial task, considerable insight into the physical phenomena involved can be gained by considering a simple one-dimensional problem with square well potentials as that depicted schematically in the inset of fig. 6a. The adsorbed molecule is represented by the square well between tip and surface. This problem can be solved exactly and is formally identical to that of tunneling through quantum well structures [23]. It is obvious that the extra space contributed by the thickness of the adsorbed molecule (10 A in the figure) is not part of the tunnel barrier. For most electron energies the effect of this molecular thickness is to change the phase of the tunneling electron wavefunction which is an oscillatory function inside the molecular well, without decrease in its amplitude. This is shown in the figure where the tunneling probability calculated with the adsorbed molecular well is compared to that calculated without adsorbed well and a barrier width of 8 A, equal to the sum of the tip-to-molecule (5 A) and the molecule-to-substrate distances (3 A) (effective barrier width). For a molecule like DNA the effective barrier width will be maintained by advancing the tip a distance roughly equal to 3 A, the molecule-to-surface distance (a typical van der Waals separation). This change in tip separation is small compared to the thickness of the molecule. The schematic drawing of fig. 6b illustrates these ideas.

For some special values of the electron energy, resonant tunneling occurs that produces maxima in the calculated tunneling probability as shown in the figure . These energies correspond closely to bound states of the isolated well. The electron spends a longer time in these

"quasi-bound" states and increases its chances of tunneling into the surface. These well states correspond to the empty molecular levels of the adsorbed molecule.

4.2 The fixation to the substrate.

One serious difficulty in imaging biomolecules is that of its fixation to the substrate as our results have clearly shown. The presence of DNA on the substrate has been demonstrated by subsequent metal shadowing, while it is not easely visible to the STM [13]. There are two reasons for that. One is the weak bonding of the adsorbates to the inert substrates that are used for imaging in non-vacuum environments. The second is the strong tip-surface interaction that leads to "contact" and to the elastic deformation of the tip-substrate system. In some specific cases the repulsive contact forces have been measured to be in the range of 10^{-7} to 10^{-8} Newtons and produce local elastic deformations of the substrate of several Angstroms. This has been documented in the case of graphite [4-26] and of Re(0001) passivated by a monolayer of S [27]. This is at the origin of the so called giant corrugations in graphite [28] and of the anomalously low barrier height values found in measuring the tunneling barrier height in air in many materials. The chemically inert nature of the contacting surfaces prevents strong chemical bonding from taking place between the tip and the surface.

Our results have shown how in the case of graphite, the tip can

displace small (a few hundred A) flakes of graphite over the surface. It is not surprising then that DNA fragments on the flat graphite terraces might also be displaced when the binding force is smaller than that exerted by the moving tip. Large aggregates of DNA might be more difficult to displace by the tip and therefore can be imaged, as shown by our results and those of other authors. The other possibility is to increase the binding force of DNA to the substrate by attachment to more reactive sites like defects and step edges, as our results demonstrate. Due to these fixation problems however, the images obtained might not be representative of the average DNA fragments on the surface but only of those that either coalesce into aggregates or bind to defects.

One possible solution to these problems is to operate the microscope in a "hopping" mode, where the tip travels at a conveniently safe height over the surface and descends only to the tunneling distance during a short time to minimize contact. The results of Jericho et al. [29] demonstrate the potential of this mode of operation for weakly bound biomaterial. Another possible solution could be to use very small tunnel currents (large gap resistance) that would correspond to a sufficiently large tip-to-surface distance [12]. Another approach which could be useful is that of forming a covalent bond between the molecule and the surface through chemical treatments [30]. In view of the discussion of the last two sections, we propose that the primary effect of metal shadowing used by many authors is the fixation of the biomaterial on the surface, rather than providing electrical

conductivity to the adsorbate.

4.3 Identification.

Identification by the shape and size of the imaged objects is the procedure followed so far by most authors. Structures like that of DNA can be identified by the repeating spiral helix of the molecule. As discussed in a previous publication [16], our measured pitch of the bumps along the DNA chain varied between 27 and 50 A with an average value of 40 A. The variation observed in our measured pitch periodicity can be attributed to the fact that they correspond to isolated and dried molecules, while crystallized aggregates might conform more to the pitch periodicities measured from X-ray diffraction studies. Also the size of the DNA molecule will appear different depending on whether it is measured on isolated molecules or in crystalline aggregates. In the first case the tip size is fully convoluted and is added to the molecular width, while in closely packed rafts of DNA the periodicity or distance between molecules should not be affected by tip size effects.

Our results on the voltage dependence of image contrast provide a hint to one way to identify molecular structures through spectroscopy. Unfortunately, our knowledge of the electronic properties of the various constituents of DNA, in particular their density of states is too poor to allow any conclusion from these data at present. An interpretation of the observed effect is that at 10 meV energy the

density of states along most of the observed ring structure is very low, and so the tip is advanced towards the surface to maintain the tunnel current, with most of the advance further deforming the substrate. At 100 meV the density of states is higher and the tip is also at a greater distance. The force between tip and surface has increased sufficiently to produce a permanent damage of the ring structure during scans at 10 mV, as evidenced by the only partial recovery of the contrast in the image taken after restoring the original 100 mV bias. The loss of contrast in the image taken at 10 mV could also be due to the increased deformation of the molecule at the smaller gap resistance and unrelated to any change in the density of states.

5. Conclusions.

The main purpose of this work was to demonstrate the various important problems that are present when using the STM to image weakly bound biological material. We have shown using our results on DNA that: a) Electron transport is not a major problem. b) That considerable interaction between tip and surface is responsible for the displacement of weakly adsorbed material. This includes small graphite flakes and DNA that is not bound to other DNA molecules to form large aggregates or to defects such as step edges. c) That there is a considerable dependence of the image contrast on the bias voltage that might be used for identification.

ACKNOWLEDGEMENTS

The authors would like to thank Drs. R. Balhorn of the Lawrence Livermore National Laboratory and M. Maestre of the Lawrence Berkekely Laboratory for supplying the DNA solutions and A. Moore of Union Carbide for kindly providing the HOPG. This work was supported by the Lawrence Berkeley Laboratory through the Director, Office of Energy Research, Basic Energy Science, Materials Division of the US Department of Energy under contract number DE-AC03-76SF00098 and by the Lawrence Livermore National Laboratory under contract number W-7405-ENG-48 and by an LLNL Institutional Research and Development grant.

(a) Present address: Department of Chemistry, University of Utah, Salt Lake City, UT 84112. USA.

(b) Permanent address: Departamento de Quimica, Universidad de Sevilla. Sevilla. Spain.

REFERENCES

1. A.M. Baro, R. Miranda, J. Alaman, N. Garcia, G. Binnig, H. Rohrer, Ch. Gerber and J.L. Carrascosa. Nature 315, 253 (1985).

2. G. Travaglini, H. Rohrer, M. Amrein and H. Gross. Surf. Sci. 181, 380 (1987).

3. D.P.E. Smith, A. Bryant, C.F. Quate, J.P. Rabe, Ch. Gerber and J.D. Swalen. Proc. Nat. Acad. Sci. USA 84, 969 (1987).

4. S.M. Lindsay and B. Barris. J. Vac. Sci. & Technol. A6, 544 (1988).

5. J.S. Foster, J.E. Frommer and P.C. Arnett. Nature 331, 324 (1988).

6. D.C. Dahn, M.O. Watanabe, B.L. Blackford and M.H. Jericho. J. Vac. Sci. & Technol. B6, 548 (1988).

7. A. Stemmer, R. Reichelt, A. Engel, J.P. Rosenbush, M. Ringger, H.R. Hidber and H.-J. Guntherodt. Surf. Sci. 181, 394 (1987).

8. M. Amrein, A. Stasiak, H. Gross, E. Stoll and G. Travaglini. Science 240, 514 (1988).

9. S.M. Lindsay, T. Thundat and L. Nagahara, J. Microsc. 152, 213 (1989).

10. M.H. Jericho, B.L. Blackford, G. Southam and T.J. Beveridge. Microsc. Soc. Canada, vol XVI, 6 (1989).

11. J. Ford, D.P. Allison, J.S. Cook, T.L. Ferrell, K.B. Jacobson, J.G. Montovani, B. Reddick and R. J. Warmick. Preprint.

12. A. Stemmer, A. Hefti, U. Aebi and A. Engel. Preprint.

13. D. Kelly, R.W. Kelly and C. Bustamante. Ultramicroscopy (preprint). See also these proceedings.

14. G. Lee, P.G. Arscott, V.A. Bloomfield and D.F. Evans. Science, 244, 475, (1989).

15. P.G. Arscott, G. Lee, V.A. Bloomfield and D.F. Evans. Nature, 339, 484, (1989).

16. T.P. Beebe, Jr., T.E. Wilson, D.F. Ogletree, J.E. Katz, R.

Balhorn, M.B. Salmeron and W.J. Siekhaus, Science, 243, 370 (1989).

17. M. Amrein, R. Durr, A. Stasiak, H. Gross and G. Travaglini. Science, 243, 1708 (1989).

18. S.M. Lindsay, T. Thundat, L. Nagahara, U. Knipping and R.L. Rill. Science, 244, 1063 (1989).

19. J.A.N. Zasadzinski, J. Schneir, J. Gurley, V. Elings and P.K. Hansma. Science 239, 1013 (1988).

20. M. Salmeron, D.S. Kaufman, B. Marchon and S. Ferrer. Appl. Surf. Sci. 28, 279 (1987).

21. J.W. Lyding, S. Skala, J.S. Hubacek, R. Brockenbrough and G. Gammie. J. Microsc., 152, 371 (1988).

22. The electronic control and software is commercially available from RHK Technology, Rochester Hills, MI. The STM head is available commercially from McAllister Technical Services, Berkeley, CA.

23. E.E. Mendez, in "Physics and Applications of Quantum Wells and Superlattices". Ed. E.E. Mende and K. von Klitzing. Plenum Publ. Corp., p. 159 (1988).

24. H. Yamada, T. Fuji and K. Nakayama. J. Vac. Sci. & Techmol. A6, 293 (1988).

25. C.M. Mate, R. Erlandsson, G.M. McClelland and S. Chiang. Surf. Sci. 208, 473 (1989).

26. H.J. Mamin, E. Ganz, D.W. Abraham, R.E. Thomson and J. Clarke. Phys. Rev. B 34, 9015, (1986).

27. M. Salmeron, C. Ocal, D.F Ogletree, T. Beebe and W. Siekhaus. March Meeting of the APS. St. Louis, 1989. Bull. Am. Phys. Soc. 34, 670 (1989).

28. J.B. Pethica, Phys. Rev. Letters. 57, 3235 (1986).

29. M.H. Jericho, B.L. Blackford and D.C. Dahn, Scanning Tunneling Microscope Imaging Technique for Weakly Bonded Surface Deposits. Preprint.

30. W.M. Heckl, K.M.R. Kallury, M. Thompson, C. Gerber, H.J.K. Horber and G. Binnig, "Characterization of a Covalently-bound Phospholipid on a Graphite Substrate by XPS and STM". Preprint.

FIGURE CAPTIONS

Fig. 1. Topographic images of graphite showing defect structures. a) 2000x2000 A area with notched step and folded-back bilayer flake. b) 2500x2500 A area showing flakes detached from step edges. Sample bias -0.1 V. Gap resistance 100 Mohm.

Fig. 2. Fine structure of some step edges in graphite without (a) and with (b) DNA deposited. a) 600x575 A image showing structures with 20 A periodicity. Bias -0.1 V. Gap resistance 30 Mohm. b) 2480x2415 A area showing edges of triangular flakes. Periodicities of 78 A are observed. Bias -0.04 V. Gap 85 Mohm.

Fig. 3. a) 1000x1000 A image showing a large terrace on the upper left side and a small flake on the right 150x250 A size. b) Same area after second scan showing displacement of the graphite flake to the left. Discontinuities are due to smaller displacements during scanning. c) 18x19 A scan taken on top of a 200x200 A flake showing elongated unit cells, (4 A in one direction and 7 A in the other) due to the tip dragging the flake as it scans. Gray scale range 1.85 A. Bias -0.1 V. Gap 100 Mohm.

Fig. 4. Sequence of images of isolated DNA strands bound to graphite flake edges showing tip displacement effects. Two small sudden displacements of central oval structure during the scan are

observed in a). Less strongly bound material in left of a) (470x470 A), bottom of b) (400x470 A) and left of c) (425x400 A) is displaced out of the area in successive scans. Part of the oval structure in a) b) and c) appears at top right corner of d) (480x400 A) and e) (600x600 A). Notice evolution of DNA fragment at bottom part in d), e) and f) (400x400 A). The sequence of bumps in this and in the oval structure are interpreted as due to the DNA spirals. Bias -0.1 V. Gap 1 Mohm.

Fig. 5. Bias effects in circular fragment after deposition of calf thymus DNA on graphite. a) Image taken at a sample bias of -0.1V. Average height of ring is 25 A. b) Same area at a sample bias of -0.01V. Only some fragments of the ring are visible. Notice also height has decreased to 6 A roughly. c) Same area after restoring -0.1V bias. Contrast over most of ring is recovered but height is irreversibly lost. Tunnel current 1 nA in a) and c) and 0.5 nA in b).

Fig. 6. (a) Calculated one-dimensional tunneling probability for the square well potential shown in the inset as a function of electron energy from the bottom to the top of the well. The left and right semiinfinite wells represent the tip and surface and the middle 10 A wide well, an adsorbed molecule. The three maxima correspond to resonant tunneling with bound states of the isolated central well. For comparison, the corresponding curve for simple tunneling through an 8 A wide barrier is also shown. (b)

Schematic diagram showing the trajectory of the tip as it scans from the bare surface to over a weakly adsorbed molecule. The tunneling barrier regions are shown hatched. The thickness of the molecule does not contribute to the barrier width.

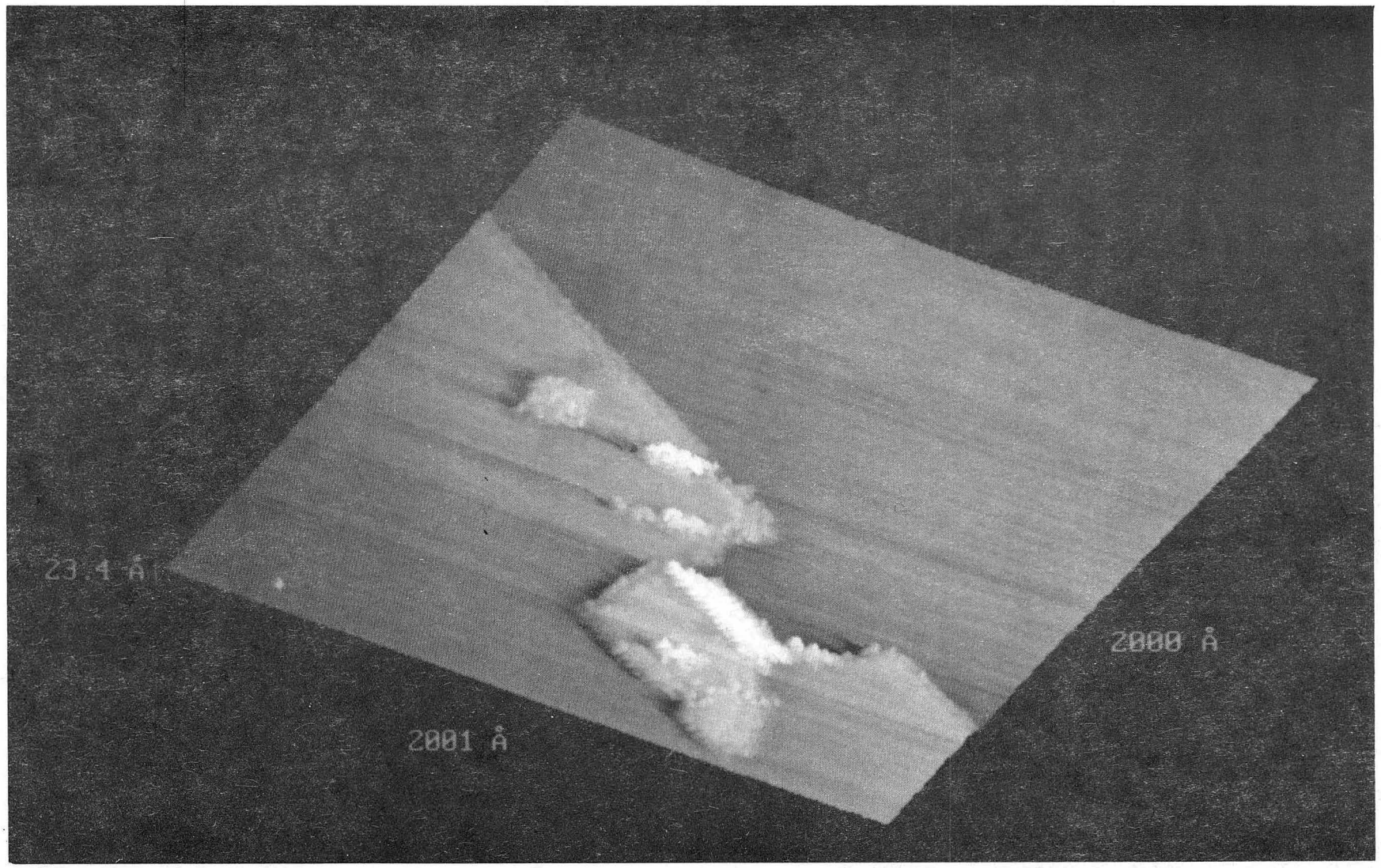

CBB 893-1783

Fig. 1a

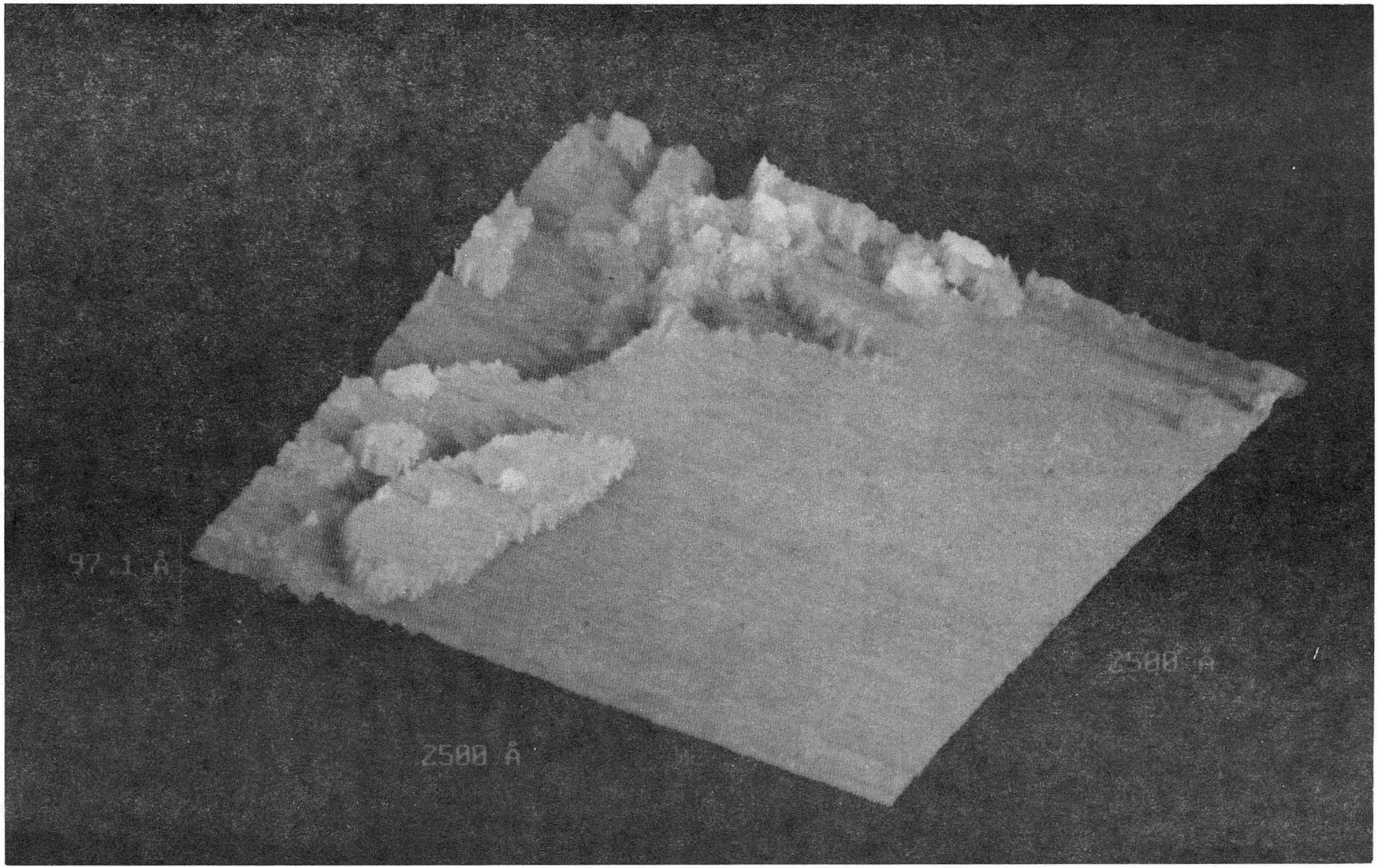

CBB 893-1779

Fig. 1b

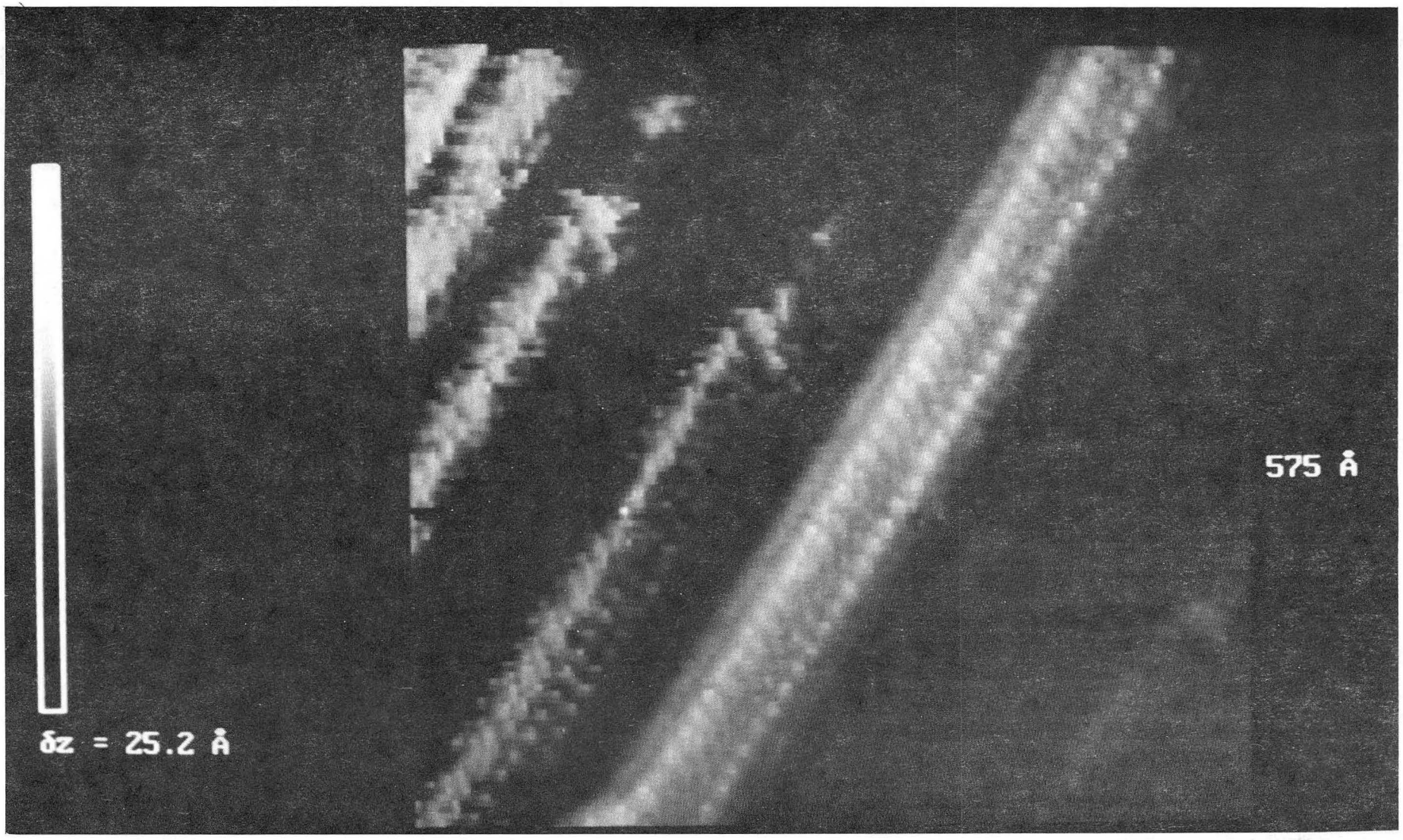

CBB 893-1857

Fig. 2a

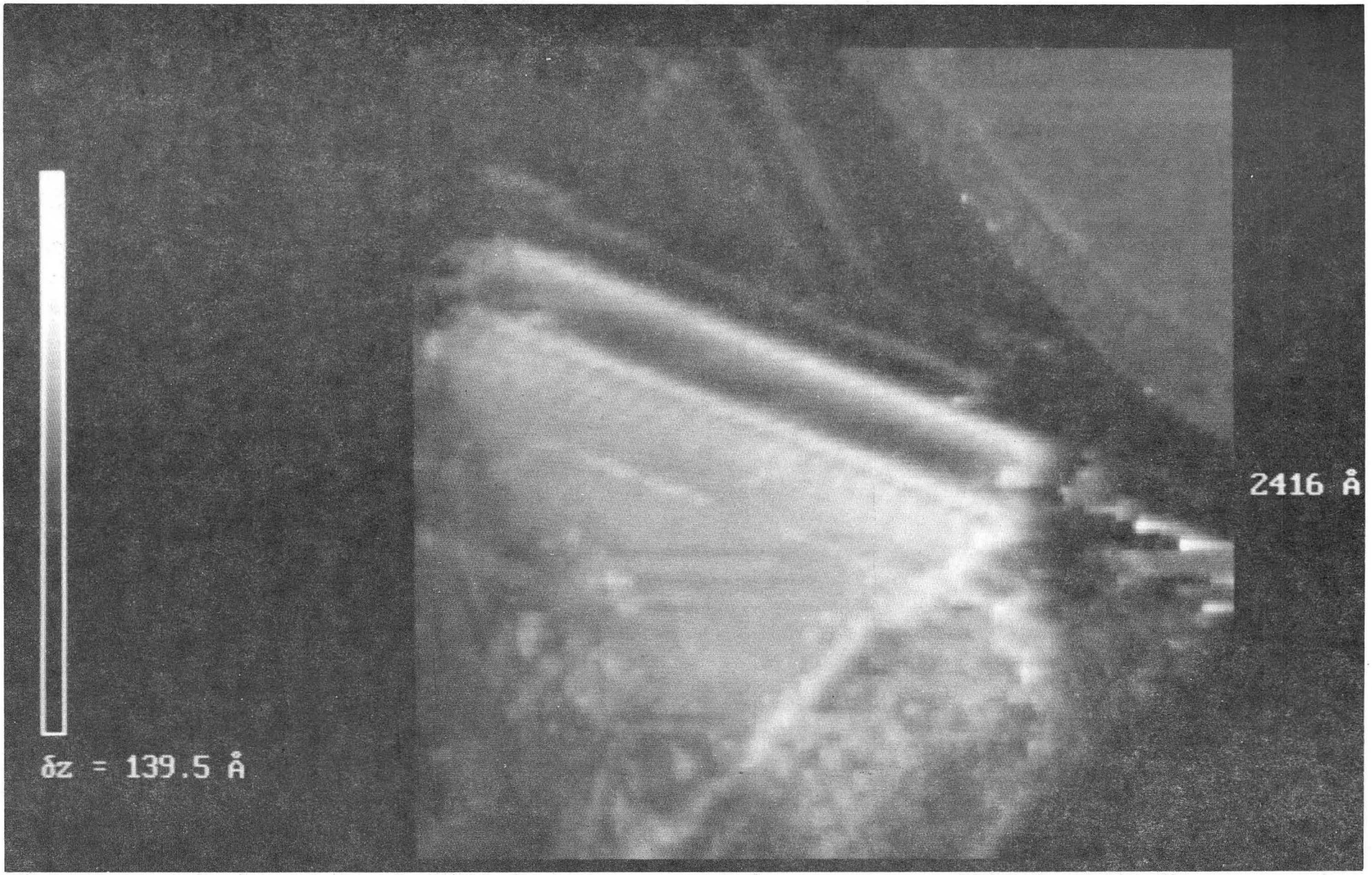

XBB 896-5175

Fig. 2b

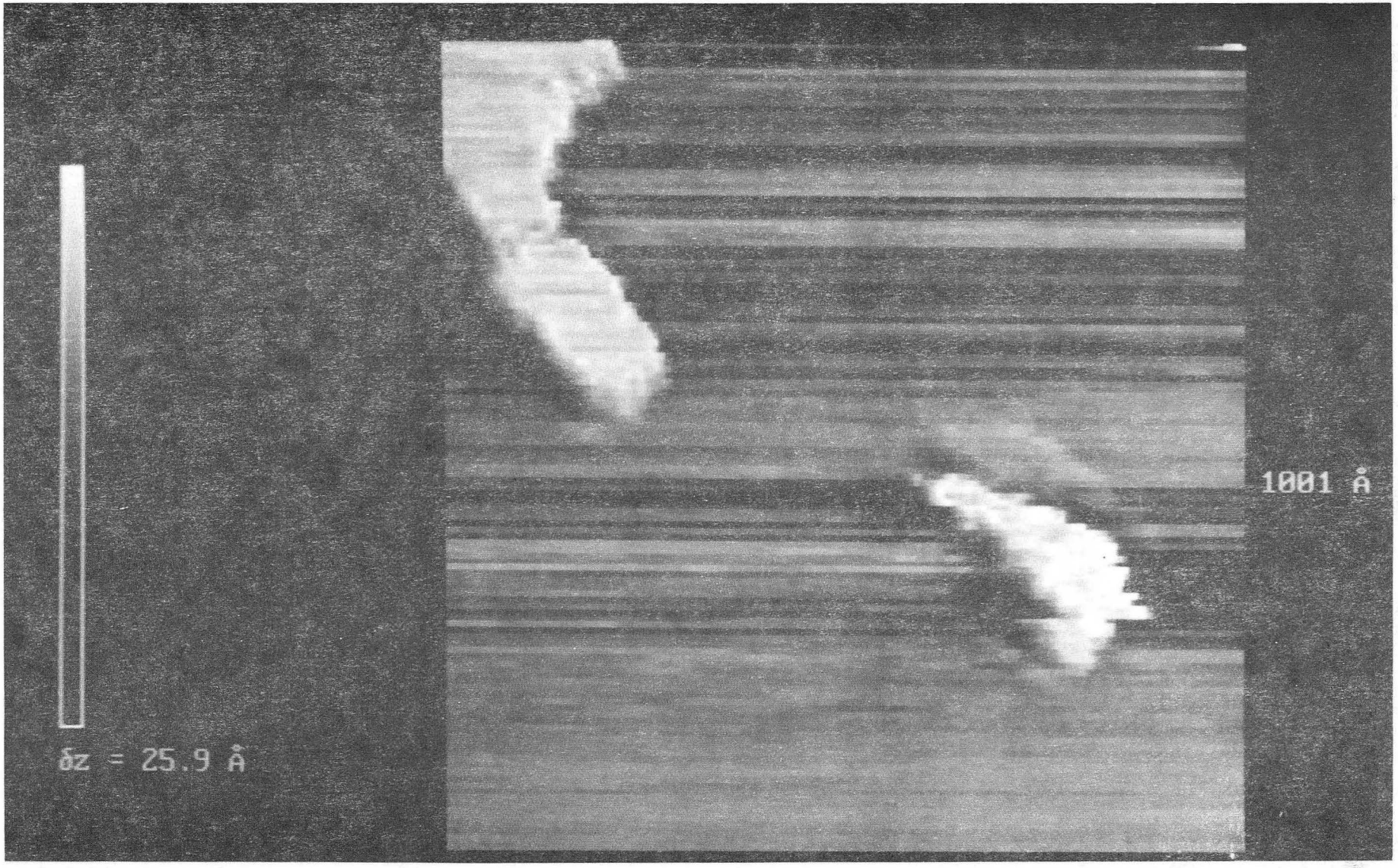

XBB 896-5168

Fig. 3a

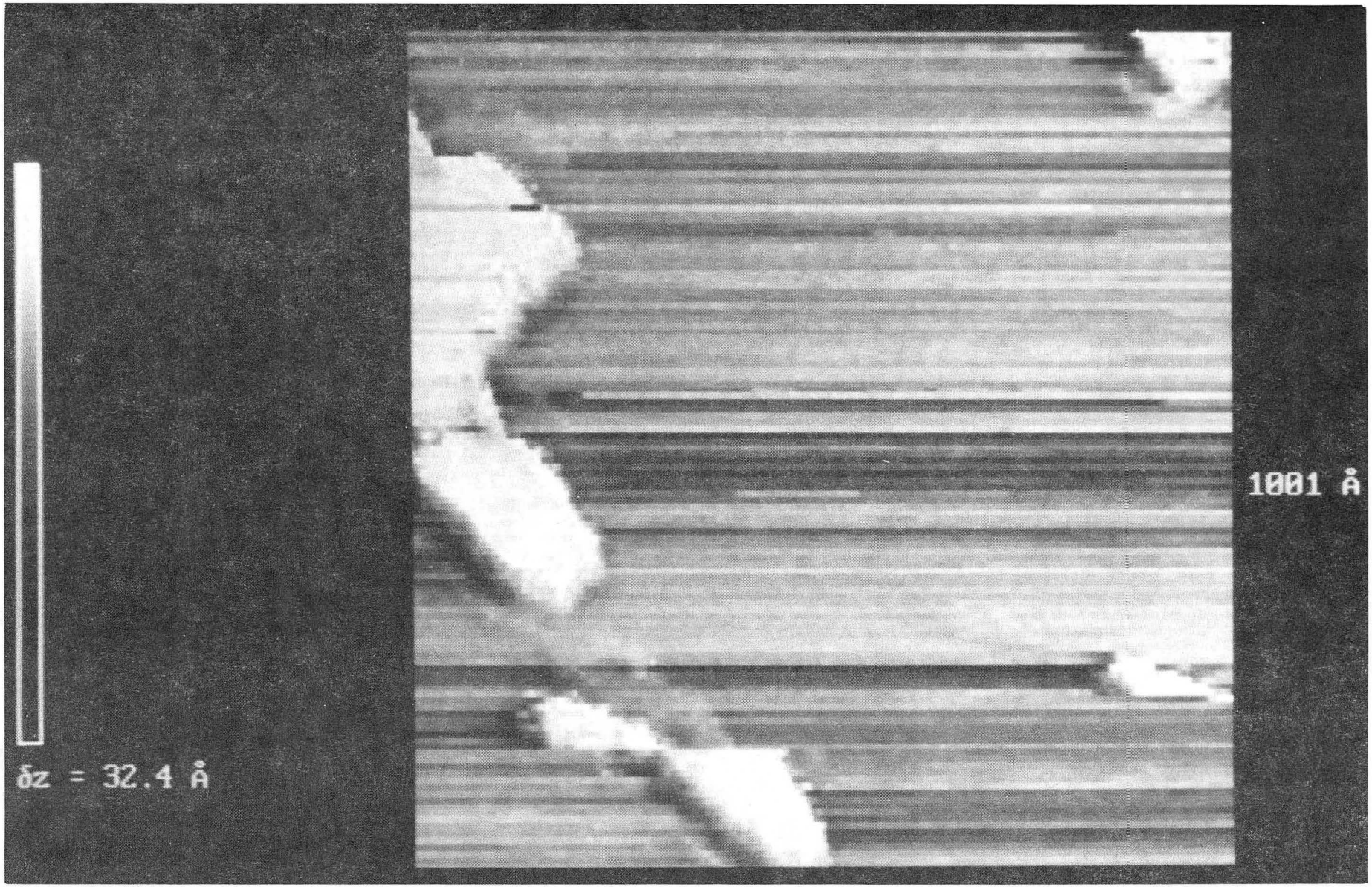

XBB 896-5169

Fig. 3b

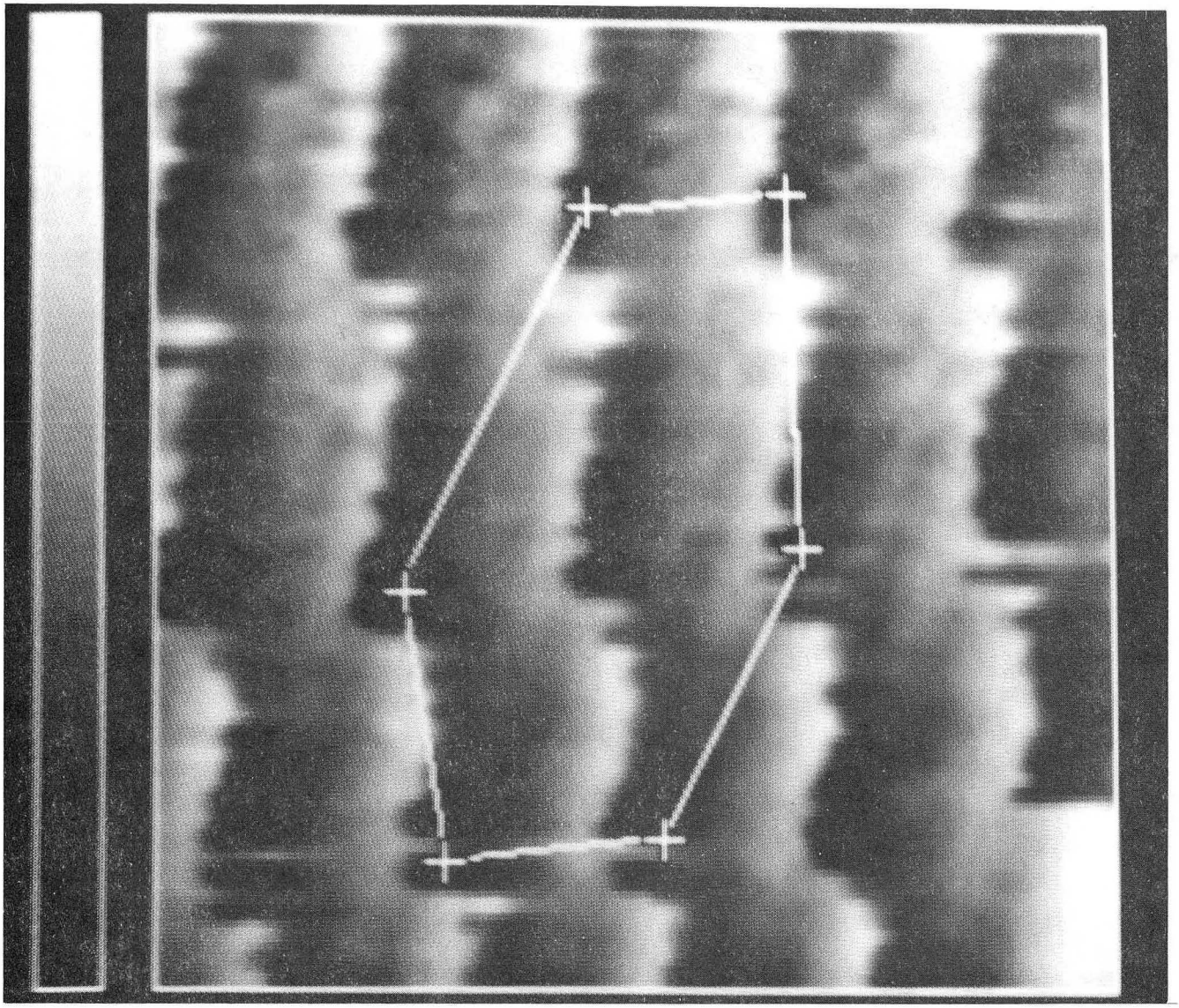

XBB 896-5171

Fig. 3c

CBB 893-1841

Fig. 4a

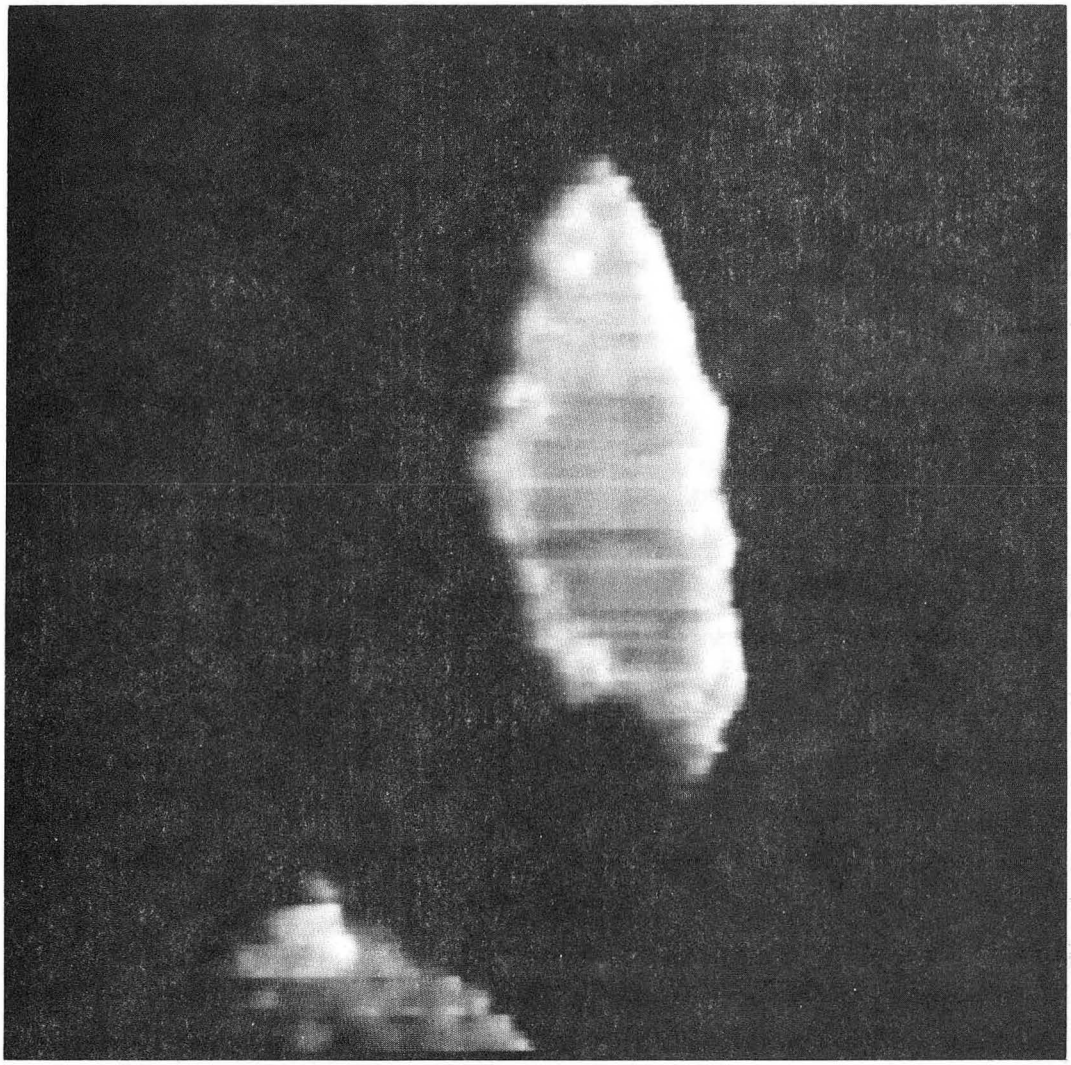

CBB 893-1845

Fig. 4b

CBB 893-1843

Fig. 4c

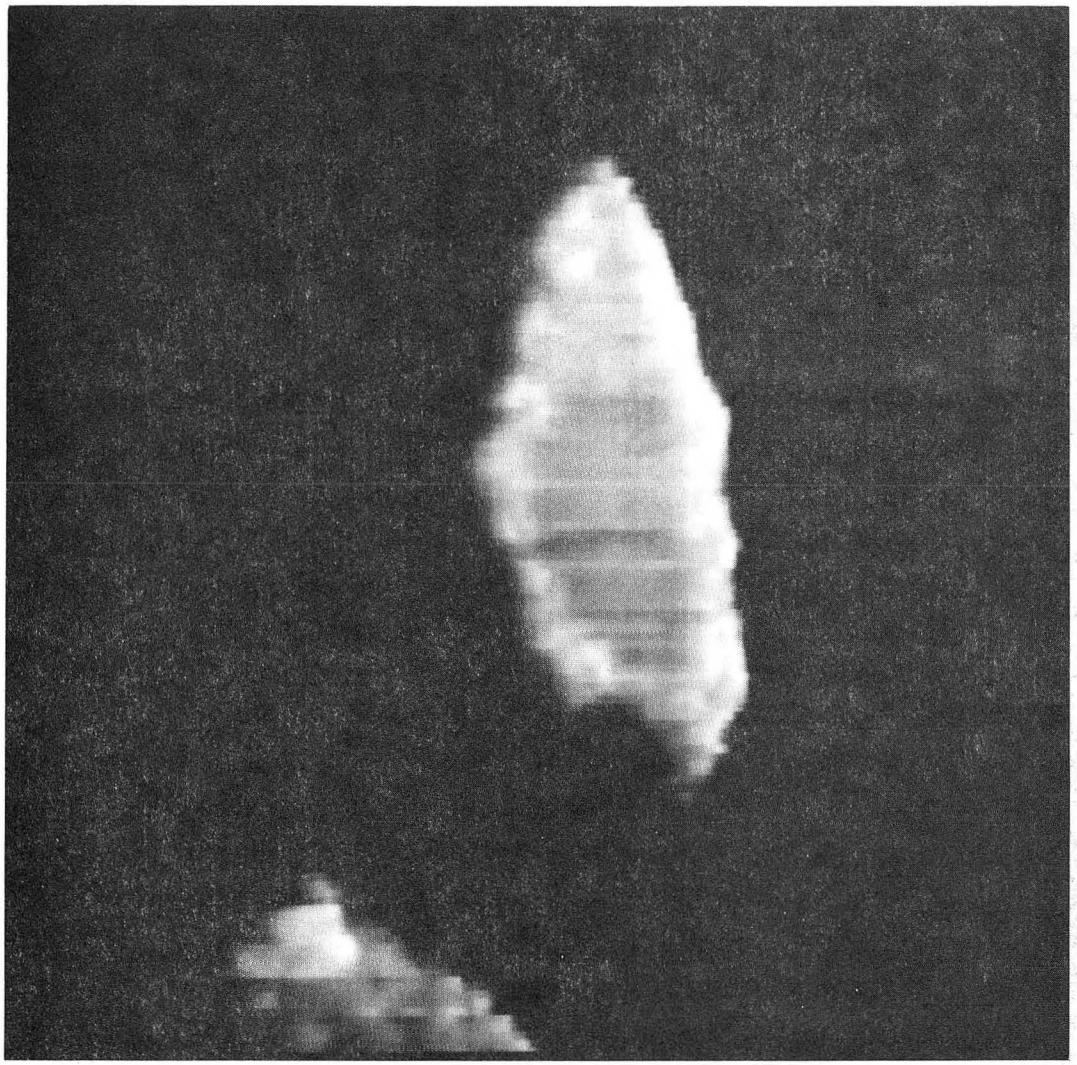

CBB 893-1845

Fig. 4b

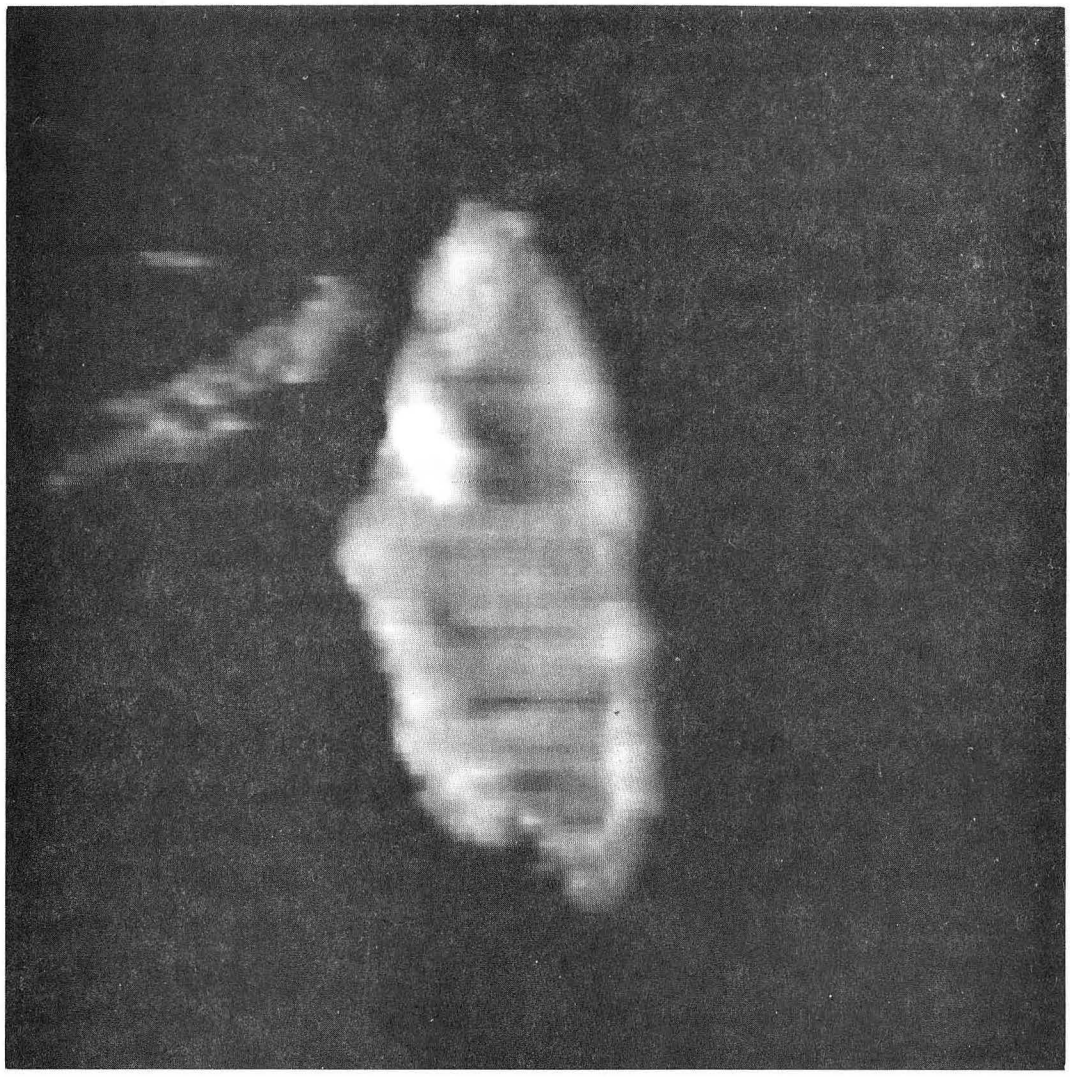

CBB 893-1843

Fig. 4c

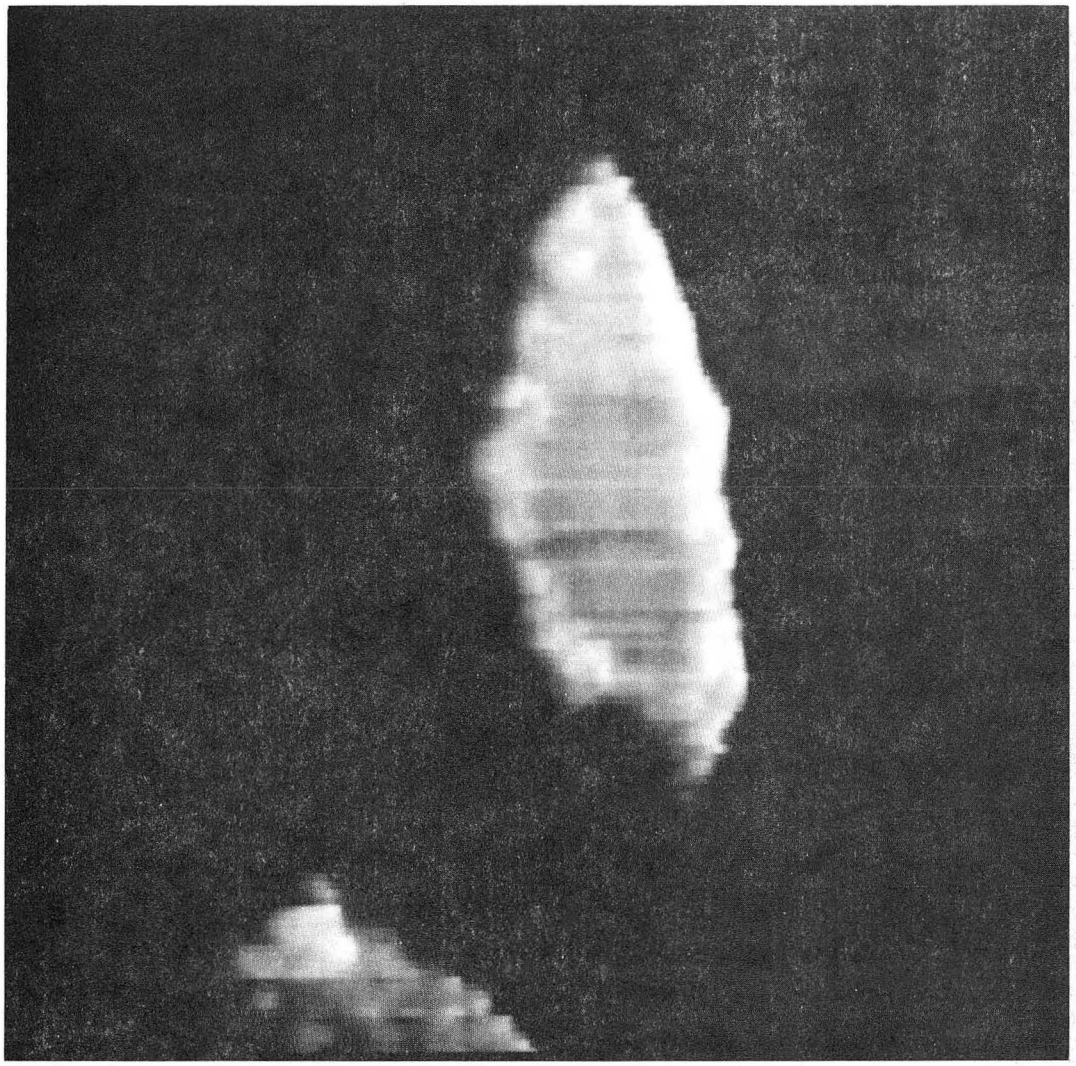

CBB 893-1845

Fig. 4b

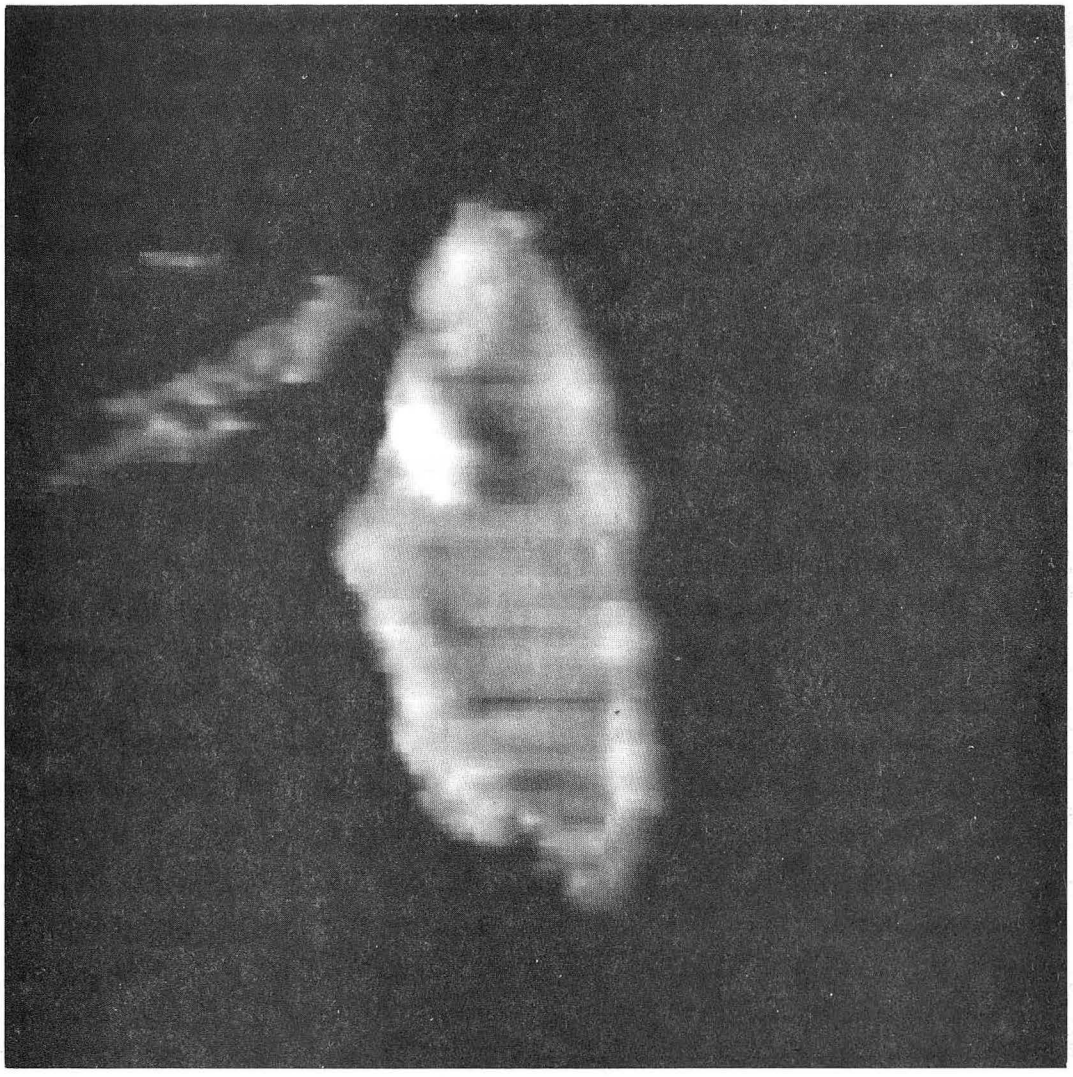

CBB 893-1843

Fig. 4c

CBB 893-1853

Fig. 4d

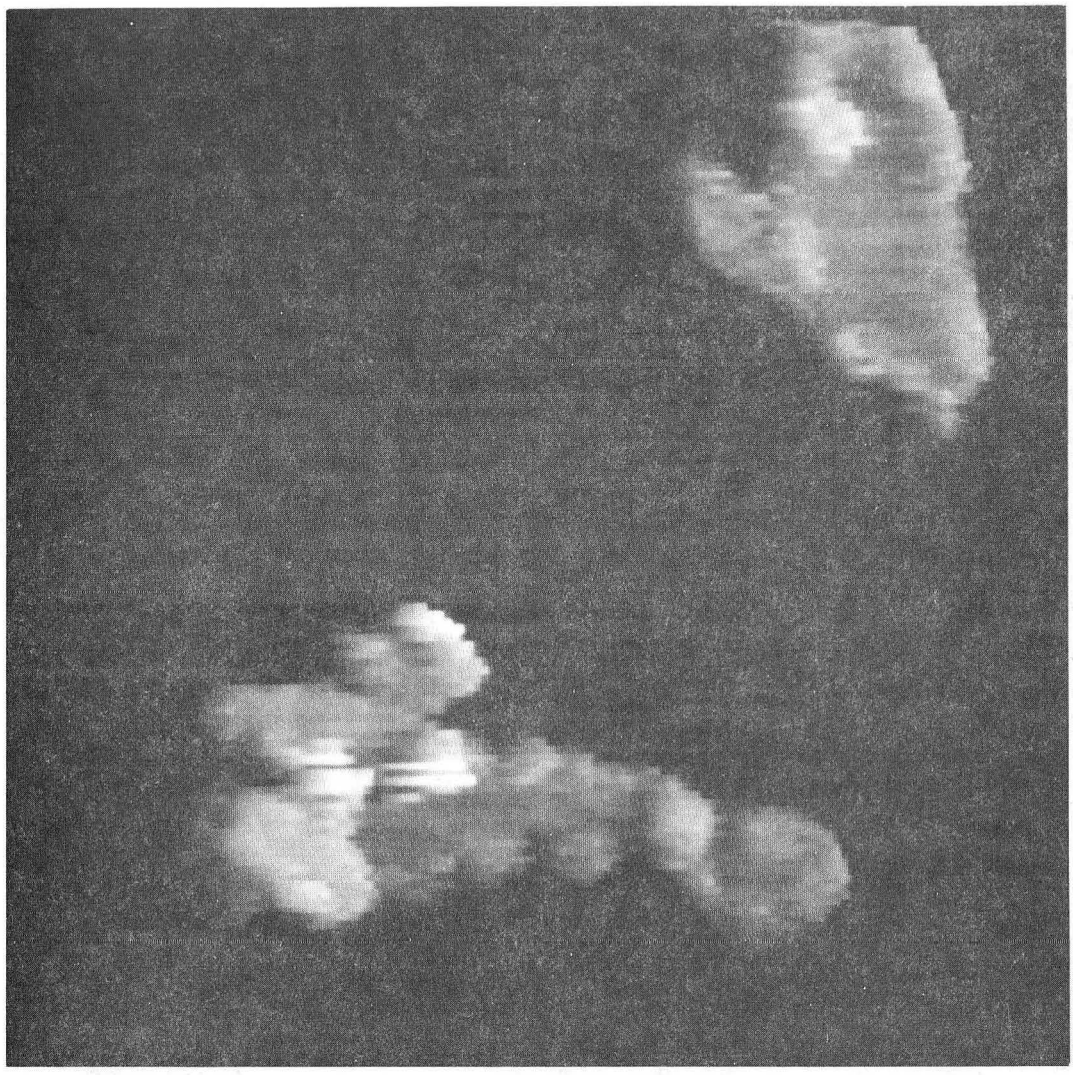

CBB 893-1851

Fig. 4e

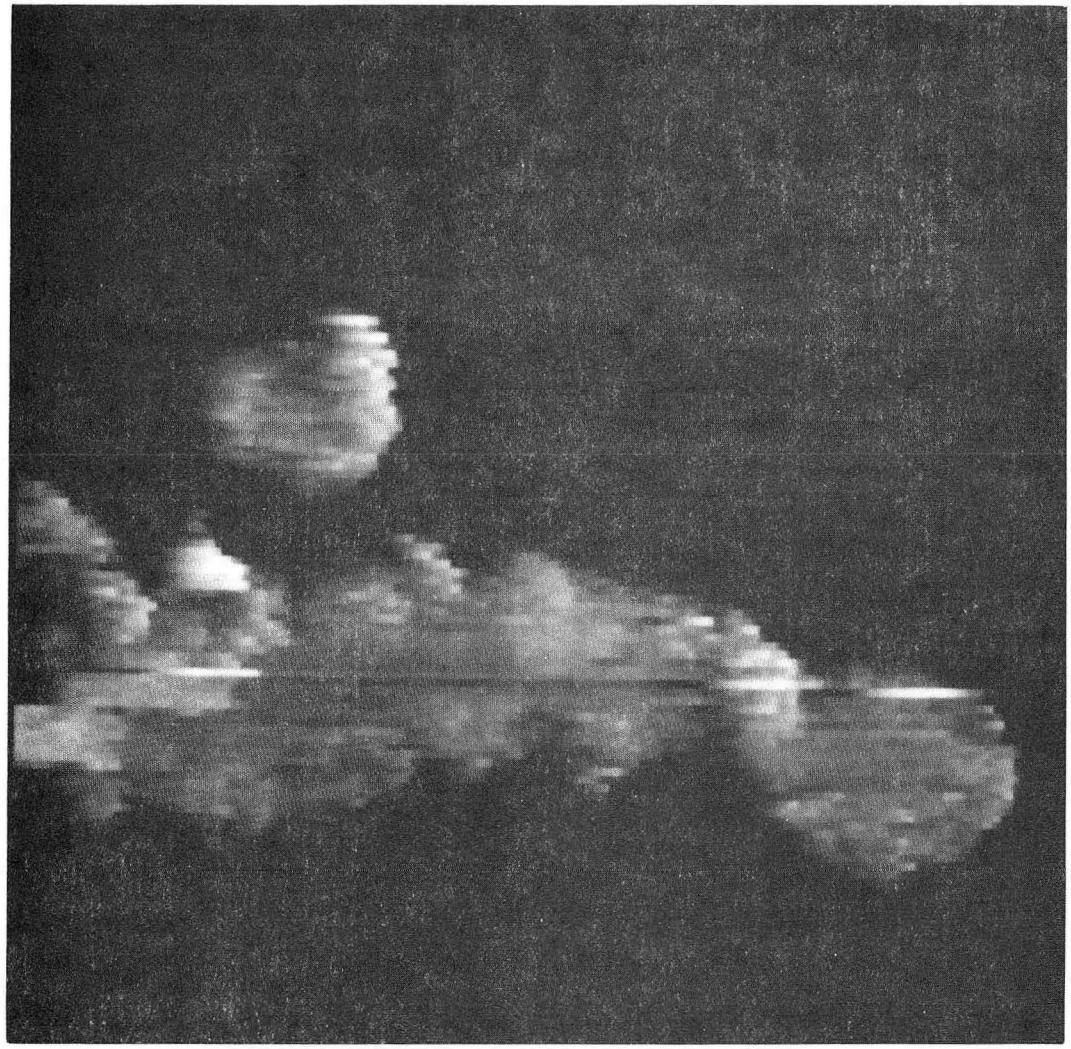

CBB 893-1847

Fig. 4f

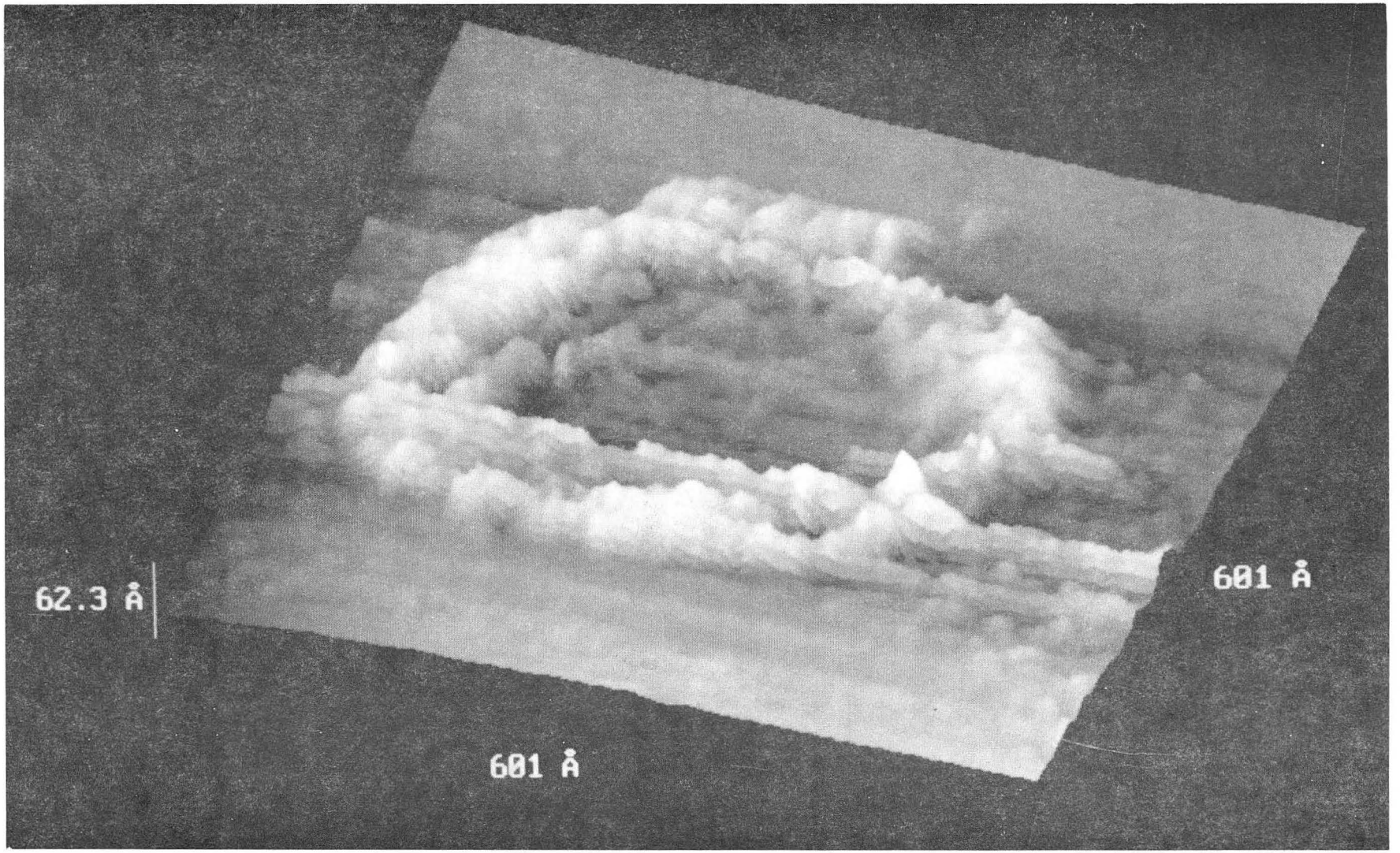

CBB 893-1821

Fig. 5a

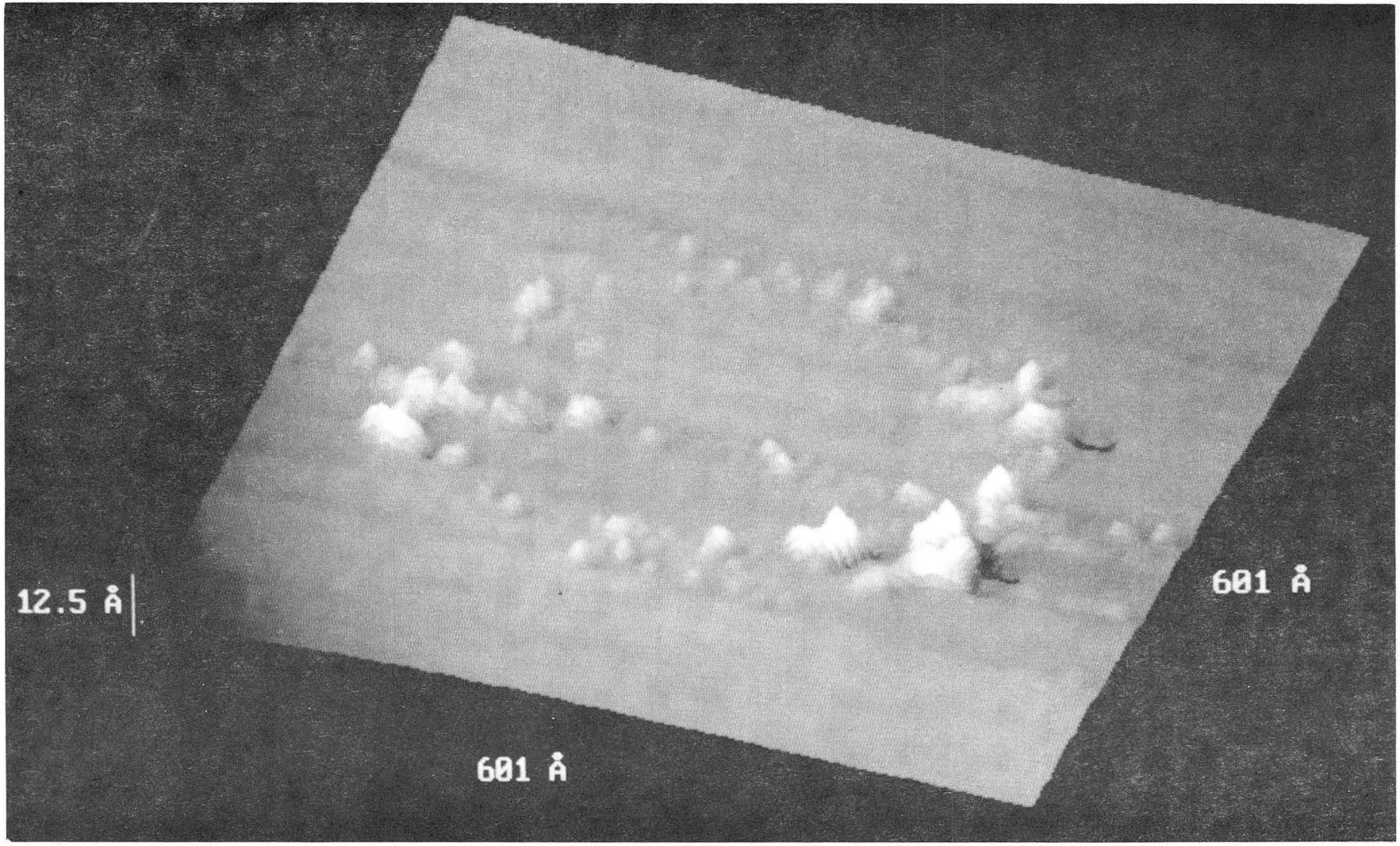

CBB 893-1809

Fig. 5b

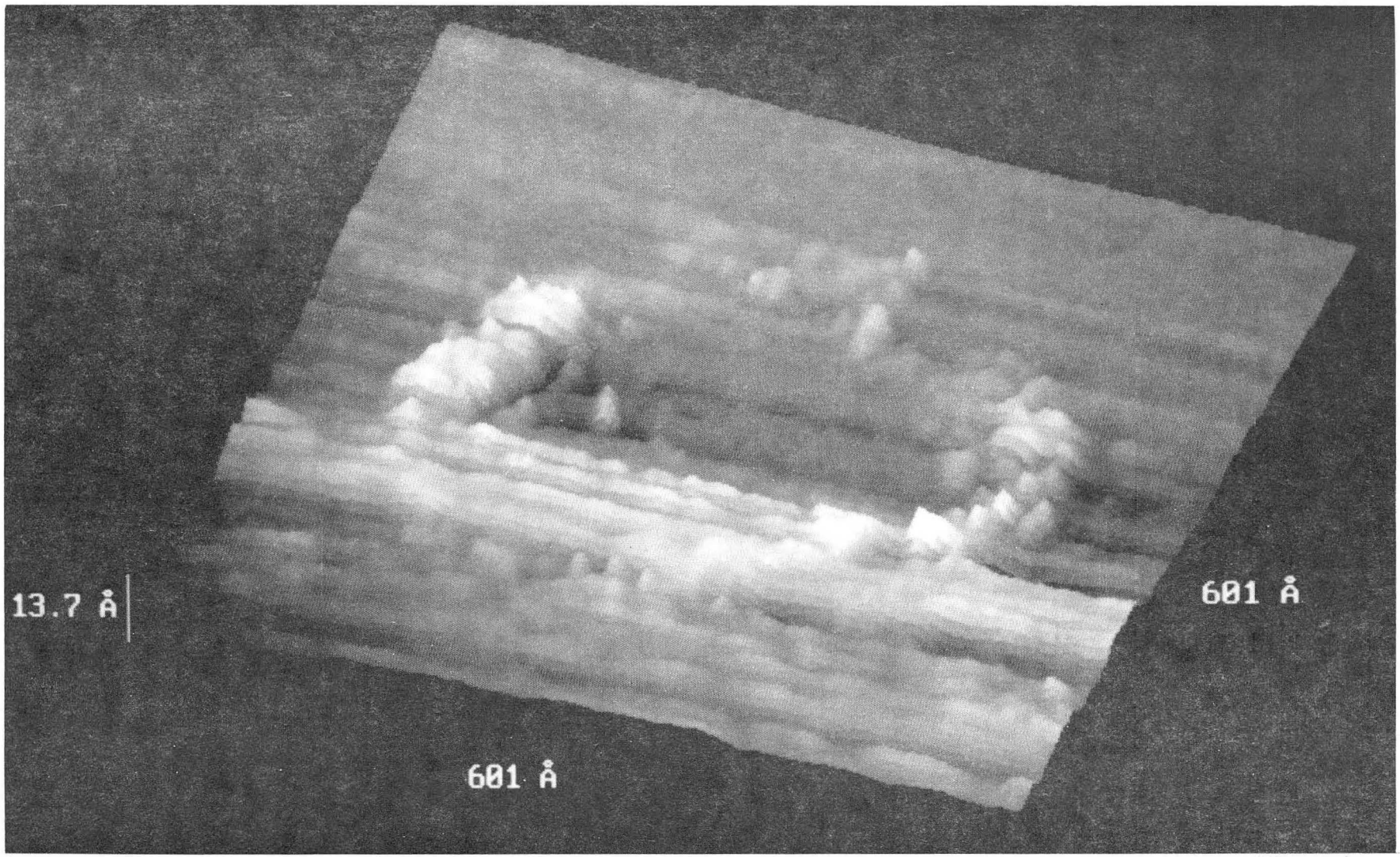

CBB 893-1831

Fig. 5c

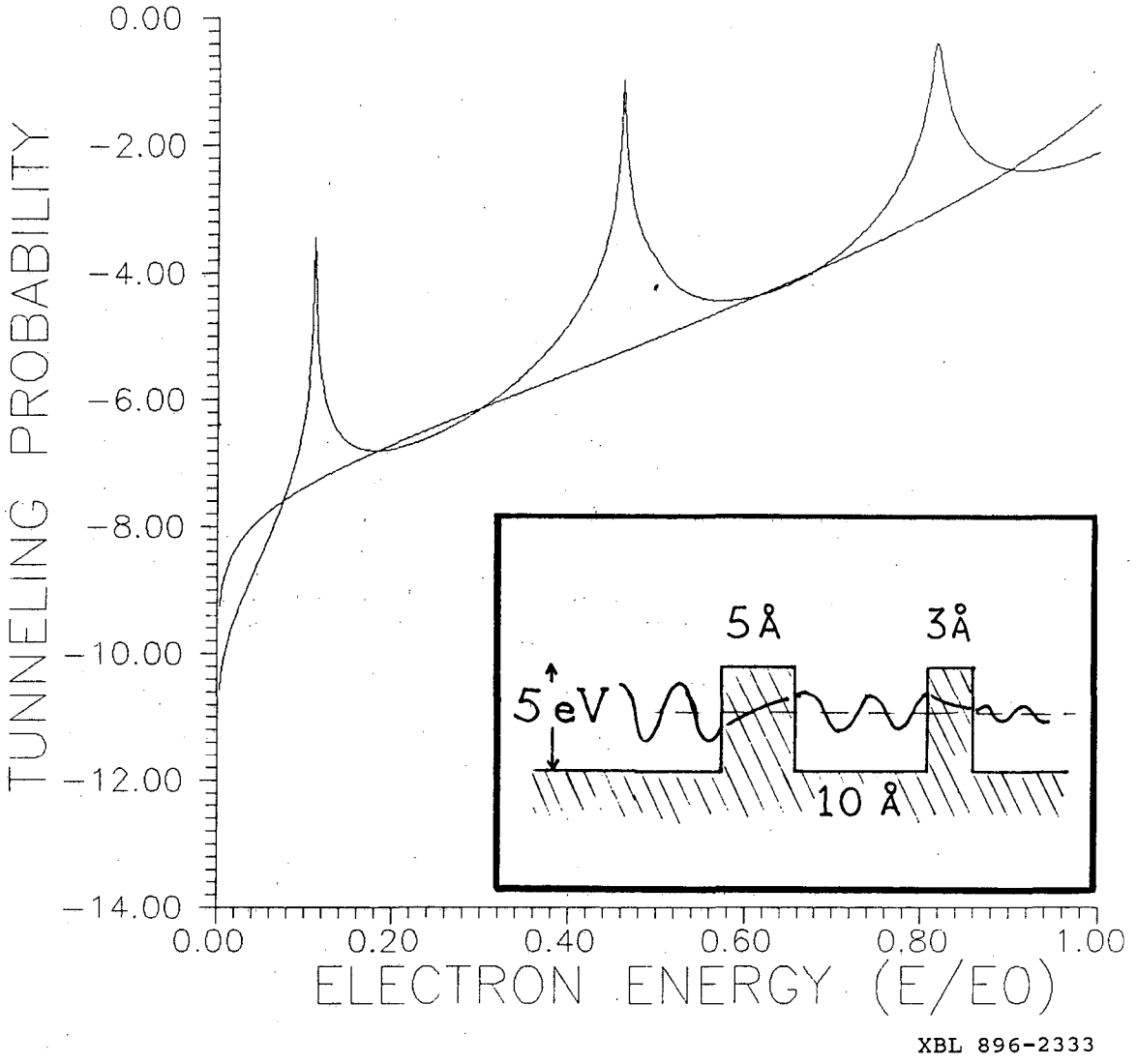
0.00
-2.00
-4.00
-6.00
-8.00
-10.00
-12.00
-14.00
TUNNELING PROBABILITY
0.00
0.20
0.40
0.60
0.80
1.00
ELECTRON ENERGY (E/E0)
5Å
3Å
5 eV
10 Å
XBL 896-2333

Fig. 6a

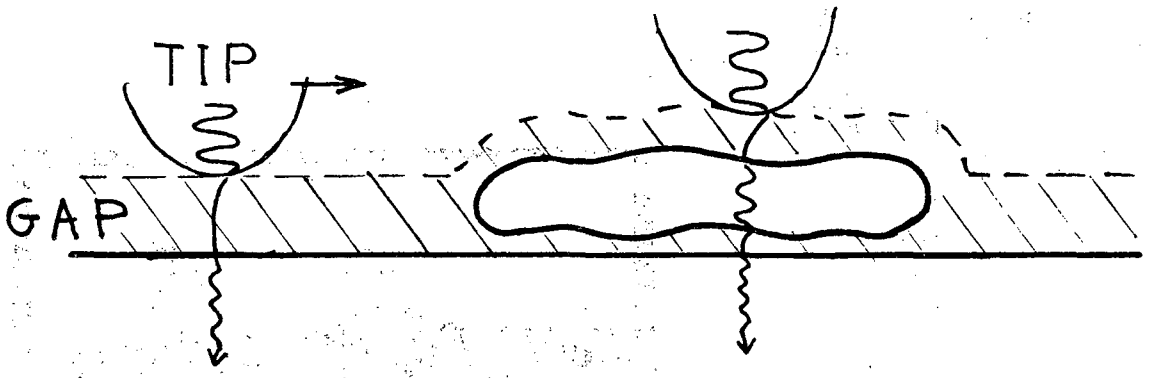

XBL 896-2332

Fig. 6b

LAWRENCE BERKELEY LABORATORY
CENTER FOR ADVANCED MATERIALS
1 CYCLOTRON ROAD
BERKELEY, CALIFORNIA 94720